

THE EFFECT OF SUBSTITUTION OF Fe BY Co ON RAPIDLY QUENCHED (FeCo)MoCuB AMORPHOUS ALLOYS

Marek Paluga, Peter Mraňko, Peter Švec, Dušan Janičkovič, Emília Illeková

Institute of Physics, Slovak Academy of Sciences, Dúbravská cesta 9, 845 11 Bratislava

Clara. F. Conde

Dept. of Physics of Condensed Matter, Faculty of Sciences, University of Sevilla, Spain

Summary $(\text{Fe}_{1-x}\text{Co}_x)_{79}\text{Mo}_8\text{Cu}_1\text{B}_{15}$ amorphous alloys were prepared in the form of ribbons by rapid quenching for $x=0, 0.25$ and 0.5 . The effect of variation of Co/Fe ratio is analyzed with respect to the formation of amorphous state and to transformation of the structure into nanocrystalline phases formed after subsequent thermal treatment. Selected properties and atomic structure in as-quenched state are studied by TEM, AFM, XRD and by measurement of magnetoresistance characteristics. The influence of heat treatment on transport and magnetic properties is shown on temperature dependencies of electrical resistivity and magnetization. It was found that while the increase of Co content leads to the increase of Curie temperature of as-quenched structure, transition to nanocrystalline state is not affected in a significant manner. The as-quenched state for alloy without Co was found to contain thin crystal-containing layer which, however, was observed, contrary to general behavior, at the side of the ribbon exposed to higher quenching rates.

1. INTRODUCTION

Formation and transformation behavior of amorphous Fe-Mo-B based alloys were studied recently [1] in form of thin films prepared by electroless plating. The effect of addition of small amount of Cu on structural and magnetic properties of rapidly quenched amorphous $\text{Fe}_{76}\text{Mo}_8\text{Cu}_1\text{B}_{15}$ was investigated in detail by Mössbauer spectroscopy, differential scanning calorimetry (DSC), X-ray diffraction (XRD), transmission electron microscopy (TEM), high resolution electron microscopy (HREM) [2, 3]. The results obtained suggested a possibility to enhance significantly certain properties by substituting a suitable metallic element in place of Fe.

In this work we have studied the influence of the addition of cobalt into Fe-Mo-Cu-B system by using different measuring techniques and microscopic methods.

2. EXPERIMENTAL DETAILS

Amorphous $(\text{Fe}_{1-x}\text{Co}_x)_{79}\text{Mo}_8\text{Cu}_1\text{B}_{15}$ alloys for $x=0, 0.25, 0.50$ were prepared in the form of ribbons (6mm wide and $\sim 20\mu\text{m}$ thick) by the method of planar flow casting. Sample composition was checked by inductively coupled plasma spectroscopy (ICP Jobin Yvon JY-70) to be within 1% of the nominal content of each element.

Using the measurements of temperature dependencies of the electrical resistivity $R(T)$ and magnetization $M(T)$ we have obtained the most basic properties of the studied metallic system with respect to the magnetic state of as-cast systems. The complementary information has been obtained by the measurements of magnetoresistance.

TEM, atomic force microscopy (AFM) and XRD methods have provided information about structure and ordering of the constituent atoms in the bulk and on the surface of the investigated material.

The set of all experimental methods used has yielded a complex view of atomic and electronic structure of this nanocrystal-forming amorphous system.

TEM was performed on a JEOL 1200EX; samples for TEM were polished by precision ion polishing system (Gatan PIPS). AFM was performed by a PICO scanner from Molecular Imaging, Inc. XRD was performed using a standard Bragg-Brentano geometry with $\text{Cu K}\alpha$ radiation.

$R(T)$ and magnetoresistance measurements were performed by four-probe method with ultrastable current source and two Keithley nanovoltmeters controlled by PC. The $R(T)$ measurements were performed in a special planar furnace controlled by EUROTHERM 2416 controller. Heating rate was 10K/min.

Measurements of magnetoresistance were performed at 300 K using external magnetic fields in the range of 0 – 0.5 T under different mechanical loads on the sample, inducing σ -stresses between 0 and $\sim 130\text{MPa}$ on the ribbon samples. Due to rather low values of magnetoresistance thermal stabilization of the magnet-sample setup was necessary to avoid temperature drifts during measurements.

$M(T)$ measurements were performed on a Perkin-Elmer TMG 7700.

3. RESULTS AND DISCUSSION

3.1 Temperature dependent characterization

Transformation behavior in three samples with different Co/Fe ratio has been investigated by measurements of temperature dependence of magnetization $M(T)$ and electrical resistivity $R(T)$. Fig.1 shows the plots of these temperature dependencies for $x=0, 0.25$ and 0.5 .

The sample without Co ($x=0$) in the range 300K - 700K exhibits a monotonous increase of

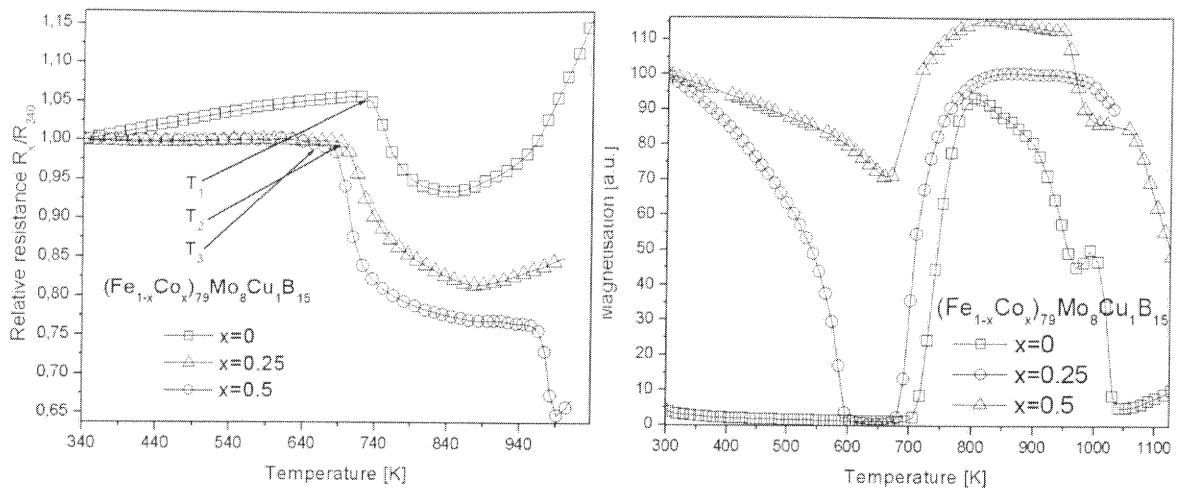


Fig.1 Electrical resistivity and magnetization of $(\text{FeCo})\text{-Mo-Cu-B}$ as-quenched amorphous samples as a function of temperature for different Co/Fe ratios; linear heating rate 10K/min.

Tab. 1 Crystallization temperature from $R(T)$ and $M(T)$, quantification of decrease of resistivity by crystallization, Curie temperature. The values are deduced from Fig. 1

sample	$T_{1,2,3}$ [K] $\{R(T)\}$	T_{cryst} [K] $\{M(T)\}$	$\Delta R/R_0$ [%]	T_{Curie} [K]
x=0	720	710	12	~290 (<290)
x=0.25	690	680	18.2	600
x=0.5	680	670	22.6	~1000

$R(T)$, which can be approximated by linear fit, yielding a temperature coefficient of electrical resistivity, TCR, of this sample in this range of $\text{TCR}=1.8 \times 10^{-4} \text{K}^{-1}$, typical for amorphous Fe-based amorphous systems. Electrical resistivity for samples with $x=0.25$ and 0.50 exhibits approximately constant value in the temperature range 300K - 640K and 300K - 680K for $x=0.25$ and for $x=0.5$, respectively; the change of $R(T)$ is in range $\pm 0.2\%$, hence $\text{TCR} \sim 0$ for these alloys in amorphous state.

The resistivity plot shows a decrease for all compositions, starting at T_1, T_2, T_3 for $x=0, 0.25$ and 0.5 , respectively, as shown in Fig. 1. The deviation from linear behavior in $R(T)$ indicates the beginning of crystallization; thus T_1, T_2, T_3 are taken as the temperatures of the onset of this process. The values are in good agreement with those obtained from $M(T)$. Crystallization terminates above $\sim 950\text{K}$ and leads to fully crystallized state.

The same qualitative transformation behaviour is observed on the $M(T)$ dependencies where a transition from a paramagnetic amorphous state into a mixture of (paramagnetic) amorphous remains and growing ferromagnetic crystalline grains lead to a sharp increase of $M(T)$ above 740K and above 700K for samples with $x=0$ and $x=0.25$, respectively. The sample with $x=0.50$ exhibits the Curie temperature above the onset of transformation, thus the increase

of $M(T)$ related to crystallization of amorphous ferromagnetic matrix is observed from values above zero. The extrapolation of $M(T)$ towards higher temperatures allows to estimate roughly the value of T_{Curie} , which may be as high as $\sim 1000\text{K}$. The increases of Curie temperature with increasing ratio of Co to Fe as well as the transformation temperatures are given in Tab. 1.

3.2 Characterization of as quenched material

Fig. 2 shows the AFM and TEM image of ribbon sample without Co. It can be seen that at the surface imaged by AFM are "cell-like", yet amorphous objects detached from each other by trench (deep $\sim 100\text{\AA}$). This effect is related to the rapid quenching process used to prepare amorphous samples and to the roughness of the quenching wheel. Inside these "cells" small crystalline grains are visible. TEM image of the sample polished from the top side of the ribbon ("air side" with respect to the rapid quenching with single roller technique) shows a view of the structure immediately below the surface. There can be seen large crystalline grains close to the surface of the "wheel" side which are replaced with increasing depth by tiny nanocrystalline grains about $\sim 5\text{nm}$ in size. Further inside the bulk or at the "air" side of the ribbon no presence of crystalline phase was detected.

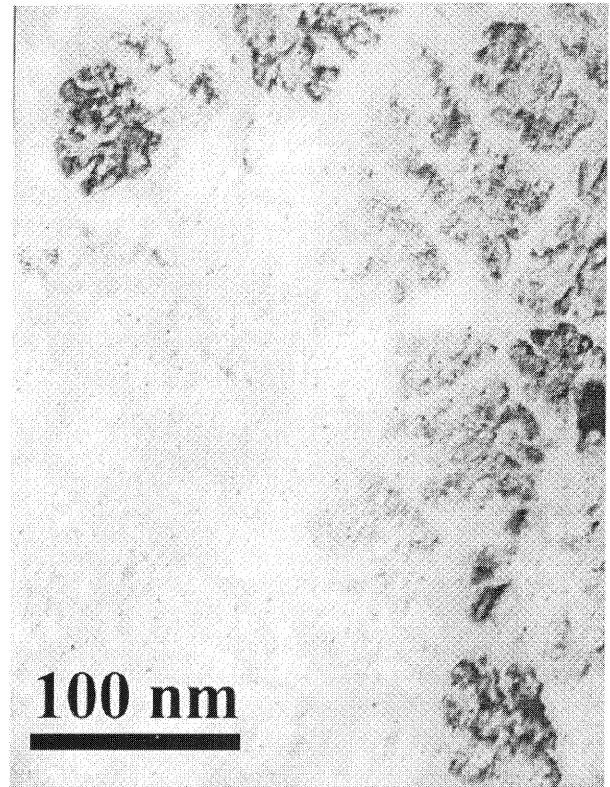
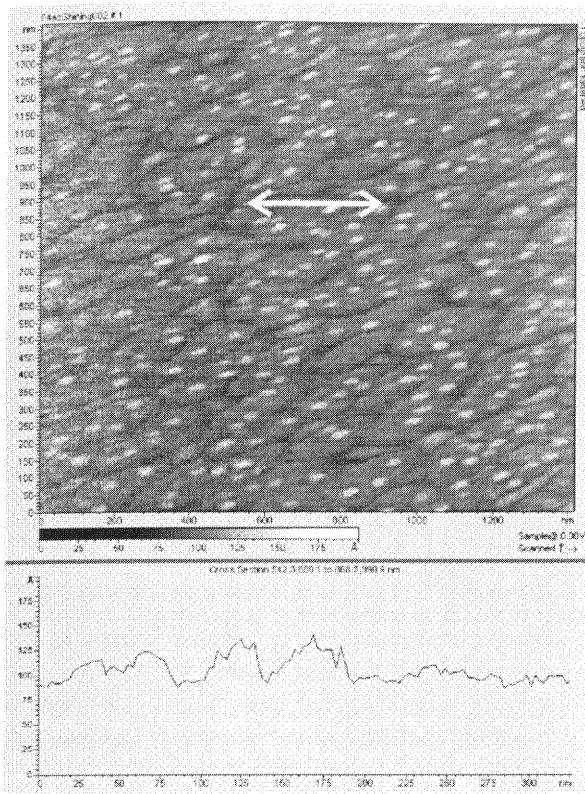


Fig. 2 Left: AFM image of sample surface with height profile from the region indicated by the marker with arrows (marker corresponds to 325nm). Picture on the right represents TEM image of the sample in the region close to the bottom surface of the ribbon; the direction towards the bulk of the sample is from the right top edge to the bottom left edge.

The presence of crystalline phase in the sample without Co is proved also by XRD. Fig. 3 shows XRD diffraction patterns for the three investigated alloys in as-quenched state. Plots 2 and 3 confirm amorphous state of the material but plot 1 shows a presence of crystalline phases at surface of amorphous material.

Fig. 4 shows two series of magnetoresistance plots. These series differ in orientation of sample against magnetic field. It could be noticed, that the orientation with surface of ribbon perpendicular to vector of homogenous planar magnetic field, shows higher magnetization field needed to reach saturation, probably due to higher demagnetization factor for this configuration. However, the character and the resistivity changes of the dependencies are the same for both orientations. Similarly as the temperature dependencies of magnetization the plots of magnetoresistance exhibit strong dependence on the content of Fe and Co.

3.3 Discussion

The plot of R(H) for $x=0$ (Fig. 4) represents the dependence of magnetoresistance of a paramagnetic system. However, the XRD pattern from the as-quenched sample (curve 1 in Fig. 3) shows two rather narrow crystalline peaks at the positions which correspond to the (110) and (220) reflections.

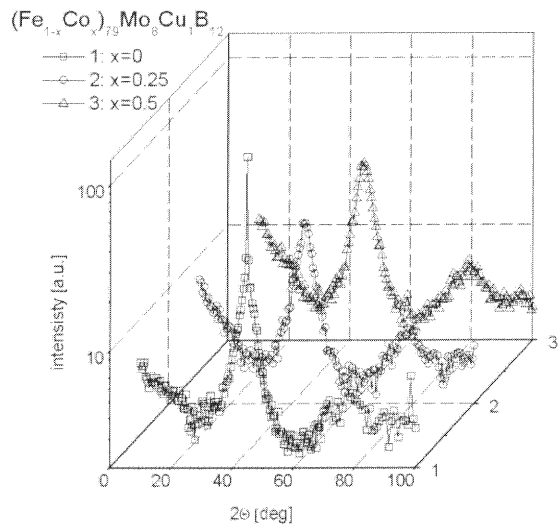


Fig. 3 XRD spectra plots of three samples in as-quenched state with different Co/Fe ratio.

of the bcc-Fe lattice. However, the reflections for (200) and (211), lying between these two, are missing. This may indicate formation of a bcc-Fe like structure which is yet not fully developed but which is the first crystalline phase formed during transformation from the amorphous state in the temperature regions as indicated by the drop of

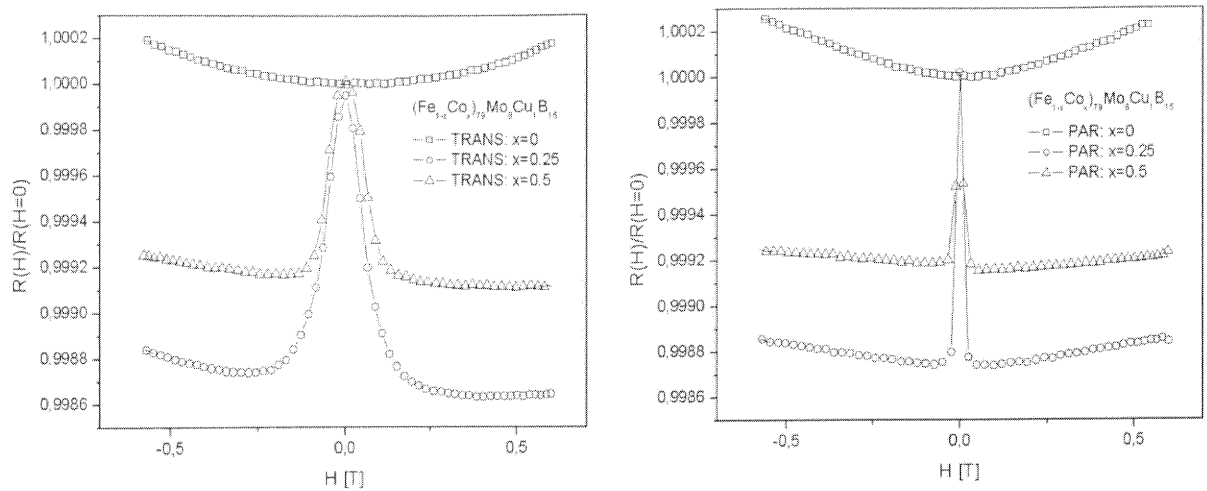


Fig. 4 The dependence of electrical resistivity on applied external magnetic field - magneto resistance plots. Plots on the right represent measurements with orientation of sample plane perpendicularly to the applied magnetic field. On the left the orientation is parallel to the magnetic field.

electrical resistivity and rise of magnetization on Fig. 1. The size and morphology of the crystalline grains observed to be present in a thin surface layer suggests that these grains are not magnetically correlated, hence the magnetoresistance exhibits paramagnetic behavior, in accord with the $M(T)$ measurements.

The ferromagnetic character of the samples with $x=0.25$ and 0.5 is evident; the electrical resistance after initial decrease reaches a saturation value for rather low applied fields, giving indication of a soft ferromagnetic system.

It is to be noted that, contrary to all previous experience, the presence of crystalline layer is observed at the bottom ("wheel") side of the ribbon, where the quenching rate is certainly higher than at the top ("air") side of the ribbon. The top side of the ribbon, however shows absolutely no presence of any crystallinity. This effect is still under investigation and it is expected that a partitioning of solutes in the precursor melt before rapid quenching or during the quenching process may be responsible for it. The effect of inverse crystalline layer present at the bottom side of the ribbon persists for compositions corresponding up to $x=0.20$, as shown in [4]

4. CONCLUSION

Substitution of iron by cobalt in Fe-Mo-Cu-B system leads to formation of fully amorphous ferromagnetic state. Increased Co content leads to increase of Curie temperature of the amorphous phase. The temperatures of transformation into nanocrystalline state, however, are not significantly affected, although the magnitude of changes of electrical resistivity increases with increasing Co content. Excellent correspondence between transformation behavior during linear heating

regimes was observed for electrical resistivity and magnetization measurements. Magnetization behavior was correlated also with measurements of magnetoresistance, showing distinct differences between paramagnetic and ferromagnetic samples. Alloys with low or no cobalt content exhibit unusual effect, where partial crystallinity is observed in the sample layer with higher quenching rate.

Acknowledgement

Support of the Slovak Grant Agencies for science (VEGA 5/5096/25, APVT-51-052702, APVT-51-021102 and SO 51/03R8 06 03) and SAS Centre of Excellence "Nanosmart" is acknowledged.

REFERENCES

- [1] W. Lingling, Z. Bangwie, Y. Ge, O. Yifang, H. Wangyu, *J. Alloys and Compounds* **255** (1997) 231.
- [2] M. Miglierini, J. Degmová, T. Kaňuch, P. Švec, E. Illeková, D. Janičkovič, *Czech J. Phys.* **54** (2004) D161.
- [3] M. Miglierini, P. Schaaf, I. Škorvánek, D. Janičkovič, E. Carpena, S. Wagner, *J. Phys.: Cond. Matter* **13** (2001) 10359.
- [4] C. F. Conde, A. Conde, D. Janickovic, P. Svec, *Journal of Magn. Mag. Mater.* (2005), submitted.